# A WIDEBAND STATISTICAL MODEL FOR NLOS INDOOR MIMO CHANNELS

*Kai Yu*[1], *Mats Bengtsson*[1], *Björn Ottersten*[1], *Darren McNamara*[2], *Peter Karlsson*[3] *and Mark Beach*[2]

[1]Department of Signals, Sensors and Systems,
Royal Institute of Technology, Stockholm, Sweden
email: kaiyu@s3.kth.se

[2]Centre for Communication Research
University of Bristol, United Kingdom

[3]Telia Research AB, Malmö, Sweden

## ABSTRACT

Herein, results of 5.2 GHz wideband indoor multiple input multiple output (MIMO) channel measurements under the EU IST SATURN project are reported. Our investigation shows that for non-line-of-sight (NLOS) cases, the average power delay profiles fit the exponentially decaying curve quite well, therefore a simple wideband model for single-input single-output (SISO) proposed in COST259 has been used in our model. Furthermore, the investigations show that the MIMO channel covariance matrix of each normalized tap of the impulse response could be well approximated by the Kronecker product of the covariance matrices seen from the transmitter and receiver respectively. Based on the above results, a wideband statistical model is presented. Monte-Carlo simulations show reasonably good agreement between the measured data and our model. Finally, we use this model to show some capacity characteristics of HiperLAN/2 channels in NLOS indoor scenarios.

## 1. INTRODUCTION

Recently, it was reported [1, 2] that channel capacity can be greatly increased by using antenna array at both the transmit and receive side as long as the environment can provide sufficient scattering. A model that could describe the MIMO channel reasonably well is a necessary requirement on designing real MIMO communication systems and therefore attracts great interest. In [3], a wideband model based on channel power correlation coefficients is presented. In [4, 5], a narrowband model has been presented for NLOS indoor scenarios based on the Kronecker structure of the channel covariance matrix. Other models can be found in [6, 7, 8]. However, most models available now are narrowband.

This paper presents the results based on 5.2 GHz measurements conducted by the University of Bristol as part of the SATURN project. We study the statistical characteristics of MIMO channel and propose a wideband model for NLOS Indoor MIMO channels based on these results. This paper is organized as follows. Section 2 makes a brief description about the measurements in Bristol. The methods used to analyze the measured data is presented in section 3. In section 4, we propose a wideband statistical model based on the measurement results and use this model to simulate the HiperLAN/2 channels. Finally, we conclude in section 5.

## 2. MEASUREMENT SETUP

The test site was the Merchant Venturers Building of the University of Bristol. The general layout of the test site includes office rooms, computer labs, corridors and open spaces. The entire measurements include 15 transmitter locations and 3 receiver locations. Both line-of-sight (LOS) and NLOS cases were measured. Note that in this paper, all the results are from NLOS cases as shown in Fig. 1. Here, the arrow at each transmitter location indicates the orientation of the transmit array. The transmitter was located in a computer lab and the receiver was located in a large modern office with cubicles.

The measurement equipment was Medav RUSK BRI vector sounder, which has an 8-element omnidirectional uniform linear array (ULA) at the transmitter side and an 8-element ULA with 120° beamwidth at the receiver side (for pictures, see [9]). The distance between two neighboring antenna elements is $0.5\lambda$ for both arrays. There is a feedback from the receiver to the transmitter by a cable maintaining the coherence between the transmitter and receiver.

THIS WORK IS CONDUCTED IN PART WITHIN SATURN (SMART ANTENNA TECHNOLOGY IN UNIVERSAL BROADBAND WIRELESS NETWORKS) FUNDED BY THE EU IST PROGRAM.

0-7803-7484-3/02/$17.00 ©2002 IEEE.

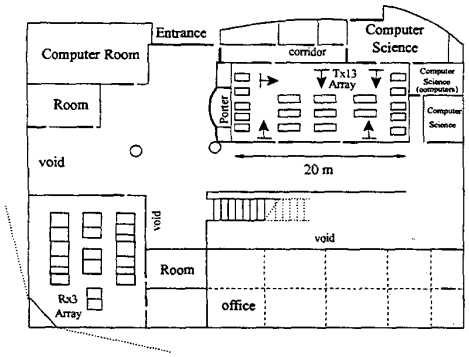


**Fig. 1**. Measurement scenario for NLOS indoor MIMO channel

The measurements were centered at 5.2 GHz. A periodic multifrequency signal with 120 MHz bandwidth was sent out by the transmitter and captured by the receiver. The channel response was then estimated and saved in the frequency domain. The maximum expected channel excess delay was $0.8\mu s$, corresponding to 97 frequency subchannels. For each transmit element, one 'vector snapshot' (one measurement from each receive element) is taken by the receiver through switching control circuits. The sampling time for each full MIMO snapshot (8 vector snapshots) is $102.4\mu s$, which is well within the coherence time of this indoor environment. One complete measurement includes 199 blocks with 16 MIMO snapshots within each block, therefore there are 3184 complete MIMO snapshots in total for each frequency subchannel. The time delay between two neighboring blocks is $26.624ms$. This means the total time for one complete measurement is $5.3s$. Finally, it is worth to mention that during the measurements, people were moving around both at the transmitter and receiver side.

## 3. ANALYSIS METHOD

### 3.1. Data Model and Channel Capacity

Assume there are $m$ transmit elements and $n$ receive elements. For a wideband MIMO channel, the input-output relationship could be expressed in the baseband as

$$\mathbf{y}(t) = \mathbf{H}_n^m(t) * \mathbf{s}(t) + \mathbf{n}(t), \quad (1)$$

where $\mathbf{s}(t)$ is the transmitted signal, $\mathbf{y}(t)$ is the received signal, $\mathbf{n}(t)$ is additive white Gaussian noise and '*' denotes convolution. The channel matrix $\mathbf{H}_n^m(t)$ here is an $n$ by $m$ channel impulse response.

It is well known [10] that when the transmitted power is equally allocated to each transmit element and frequency subband, the wideband channel capacity can be expressed as

$$C = \int_W \log_2 \det(\mathbf{I}_n + \frac{\rho}{m}\mathbf{H}(f)\mathbf{H}^H(f))df \quad \text{bits/s}, \quad (2)$$

where W is the overall bandwidth of the MIMO channel, $\mathbf{H}(f)$ is the normalized frequency response of each narrowband subchannel, $\rho$ is the average signal-to-noise-ratio (SNR) at each receiver branch over the entire bandwidth and $(\cdot)^H$ is complex conjugate transpose. Here, we use the same normalization factor for the frequency response of every narrowband subchannel such that

$$\int_W E(\| \mathbf{H}(f) \|_F^2)df = Wnm, \quad (3)$$

where $\| \cdot \|_F$ denotes the Frobenius norm and $E(\cdot)$ denotes expected value.

### 3.2. Average Power Delay Profile and RMS Delay Spread

Average power delay profile is used to show how the received power changes according to a fixed time delay reference. It is found by averaging every instantaneous power delay profile over the whole measurement time.

The rms delay spread is a measure of channel dispersive property. It is the square root of the second central moment and can be calculated as [11]

$$\overline{\sigma}_\tau = \sqrt{\overline{\tau^2} - (\overline{\tau})^2}, \quad (4)$$

where $\overline{\tau}$ is the first moment of the instantaneous power delay profile (also called mean excess delay) and $\overline{\tau^2}$ is the second moment of the instantaneous power delay profile.

### 3.3. Kronecker Structure

It was reported in [4, 5] that for a narrowband NLOS Indoor MIMO channel, the channel covariance matrix can be well approximated by the Kronecker product of the covariance matrices seen from transmit and receive side respectively, i.e.

$$\mathbf{R}_H = \mathbf{R}_H^{Tx} \otimes \mathbf{R}_H^{Rx}, \quad (5)$$

where $\mathbf{R}_H$ is the channel covariance matrix, $\mathbf{R}_H^{Tx}$, $\mathbf{R}_H^{Rx}$ are the covariance matrices at the transmitter and receiver side and '$\otimes$' denotes the Kronecker product. Suppose the channel coefficients are complex Gaussian, it is easy to show from equation (5), as in [7], that

$$\mathbf{H} = (\mathbf{R}_H^{Rx})^{1/2}\mathbf{G}[(\mathbf{R}_H^{Tx})^{1/2}]^T, \quad (6)$$

where $\mathbf{G}$ is a stochastic M by N matrix with independent and identically distributed (IID) $\mathcal{CN}(0,1)$ elements and $(\cdot)^T$ is transpose. Here $(\cdot)^{1/2}$ denotes any matrix square root

such that $\mathbf{R}^{1/2}(\mathbf{R}^{1/2})^* = \mathbf{R}$. We will revisit this structure in section 4.

For a wideband MIMO channel, it is also interesting to see whether this structure can be extended to each tap. First we define the transmit, receive and channel covariance matrices from the measured data for the $l$th tap as

$$\mathbf{R}_{Tx}^l = \mathrm{E}[(\mathbf{h}_i^H(l)\mathbf{h}_i(l))^T] \quad \text{for } i = 1, \ldots, n \qquad (7)$$

$$\mathbf{R}_{Rx}^l = \mathrm{E}[\mathbf{h}^j(l)\mathbf{h}^{jH}(l)] \quad \text{for } j = 1, \ldots, m \qquad (8)$$

$$\mathbf{R}_H^l = \mathrm{E}[\mathrm{vec}(\mathbf{H}_n^m(l))\mathrm{vec}(\mathbf{H}_n^m(l))^H], \qquad (9)$$

where $\mathbf{H}_n^m(l)$ is the $l$th tap of the channel matrix, $\mathbf{h}_i(l)$ is $i$th row of $\mathbf{H}_n^m(l)$, $\mathbf{h}^j(l)$ is $j$th columns of $\mathbf{H}_n^m(l)$ and $vec(\cdot)$ denotes the 'vec' operator.

In [5], an optimal Kronecker factorization method is proposed to factorize the channel covariance matrix $\mathbf{R}_H^l$ into two Hermitian matrices $\mathbf{X}$ and $\mathbf{Y}$. The main idea is to reorder the position of matrix elements so that the original problem boils down to a problem that can be solved by the singular value decomposition (SVD) [12]. More details could be found in [5].

The results of optimal factorization for each tap are then compared with those from the measured data in the sense of model error, which will be defined in section 4.

## 4. MEASUREMENT RESULTS

In this section, the data measured at a single pair of transmit location (Tx13) and receive location (Rx3) are used as an example. Similar results are found for the other four transmit locations. The channel impulse responses are calculated from the data using IFFT with Hanning window. It is interesting to find that the channel is quite stationary within the $5.3s$ measurement time even though people were moving around, therefore only pairs of 2 and 3 neighboring elements have been used with different subsets of elements being selected in order to get sufficiently many MIMO channel realizations.

### 4.1. Wideband SISO Model

The average power delay profile for one SISO channel is shown in Fig. 2 which looks like exponential decay. The rms delay spread is calculated by setting the threshold 20dB below the peak value of the amplitude, The cumulative density function (CDF) of the rms delay spread is shown in Fig. 3 and the mean rms delay spread in this case is $36.7ns$. The mean rms delay spread varies between 30 to $40ns$ for different transmit locations.

Based on the information of channel variation shown above, assume that the channel taps are independent zero mean complex Gaussian, we use the following simple SISO model proposed in [13] for each channel coefficient. Note that this

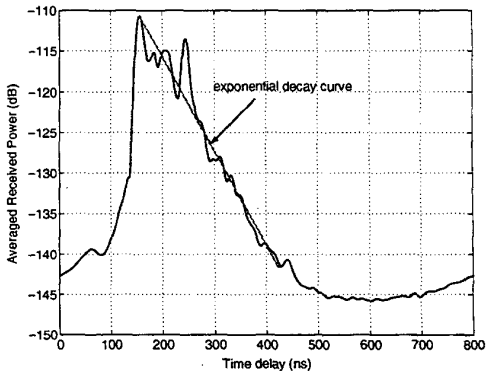


**Fig. 2**. Average power delay profile

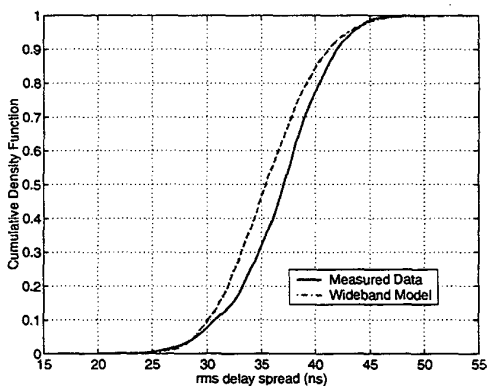


**Fig. 3**. CDF of rms delay spread of channel coefficient from measured data and wideband model

MIMO model is flexible since other SISO models can also be used.

$$h(\tau) = \sum_{l=1}^{N} a_l \delta[\tau - (l-1)\Delta\tau], \qquad (10)$$

where $l$ is label of taps, $\Delta\tau$ is the time spacing between neighboring taps, $\tau$ is delay and $a_l$ is the complex tap amplitude,

$$\bar{p}_l = A\exp[-\frac{(l-1)\Delta\tau}{2\Gamma}], \qquad (11)$$

where $\Gamma$ is the mean rms delay spread, $A$ is a normalization factor and $\bar{p}_l$ is the average power of $l$th tap. No Doppler frequency shift is considered here due to the quite stationary scenario.

### 4.2. Wideband MIMO Model

The channel covariance matrix $\mathbf{R}_H^l$ for $l$th tap (including the phase) is then calculated and compared with the Kronecker

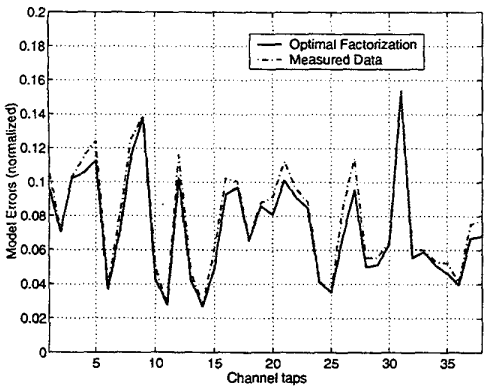


Fig. 4. Model errors of Kronecker structure (normalized)

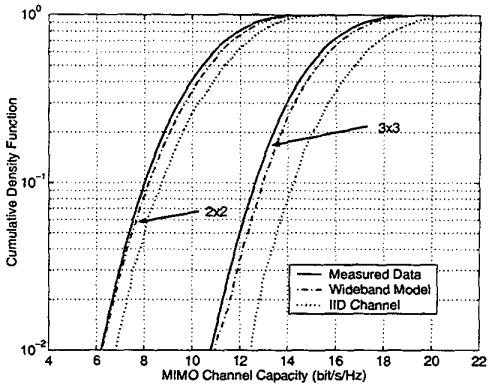


Fig. 5. CDF of narrowband channel capacity (normalized) from measured data, wideband model and IID MIMO channel. Power is equally allocated, the SNR at the receiver side is 20dB

product of the covariance matrices $\mathbf{R}_{Tx}^{l}$ and $\mathbf{R}_{Rx}^{l}$ seen from the transmit and the receive side respectively.

To measure the difference between two matrices $\mathbf{A}$ and $\mathbf{B}$, we define the following model error, $\Psi$ as

$$\Psi(\mathbf{A},\mathbf{B}) = \frac{\| \mathbf{A}-\mathbf{B} \|_F}{\| \mathbf{A} \|_F}. \qquad (12)$$

From a 2x2 case, the relative model error for each tap between $\mathbf{R}_H$ (corresponding to $\mathbf{A}$ in (12)) and Kronecker product (corresponding to $\mathbf{B}$) are presented in Fig. 4. For comparison, the model error from the optimal factorization is plotted in the same figure as well. Note that only 38 out of 97 successive taps that have higher SNR are plotted. It is shown that the mean model error is below 10% and the difference between the model error from the optimal factorization and that from the measured data is small. Therefore we conclude that for each tap, the channel covariance matrix can be approximated by the Kronecker structure reasonably well.

Combining the above SISO model and the Kronecker structure for each tap, the wideband MIMO channel matrix $\mathbf{H}(\tau)$ can be modeled as

$$\mathbf{H}(\tau) = \sum_{l=1}^{N} (\mathbf{R}_{Rx}^{l})^{1/2} \mathbf{G}_l (\mathbf{R}_{Tx}^{l})^{T/2} \delta[\tau-(l-1)\Delta\tau], \quad (13)$$

where $\mathbf{G}_l$ is the matrix with independent and identically distributed (IID) zero mean complex Gaussian elements and the average power $\bar{p}_l$ of each element can be modeled as shown in (11).

1000 MIMO channel impulse responses are generated by Monte-Carlo simulations with 2x2 and 3x3 setups. The CDF of the rms delay spread for one simulated SISO channel is plotted in the same figure as the measured data, see Fig. 3. FFT with Hanning windowing is used to transform the simulated impulse response back into the frequency domain and the capacity of the narrowband MIMO channel is calculated and compared with that from measured data (averaged in frequency domain for both cases and also over spatial domain for the measured data), see Fig. 5. Both figures show reasonably good agreement between the measured data and our wideband model.

### 4.3. Simulations of HiperLAN/2 MIMO Channels

The HiperLAN/2 standard is specified by the ETSI BRAN Project. It could provide high data rate to broadband core networks and mobile terminals. Each HiperLAN/2 channel has 20 MHz bandwidth and therefore, for a system with 120 MHz bandwidth, 6 HiperLAN/2 channels can be provided. In this section, we will use the above wideband model to generate 1000 realizations of a 120 MHz MIMO channel with 2x2 setup and the results are reported in Fig.6 and 7.

Fig.6 shows the CDF of the capacity that one 20 MHz HiperLAN/2 channel could provide. Note that 20 MHz bandwidth is fully used, no bandwidth for guard and pilot tones is considered in this paper. Only 3 out of 6 HiperLAN/2 channels have been plotted. It is shown the those channels have very similar CDF curves, which indicates that within 120 MHz bandwidth, those HiperLAN/2 channels have similar statistical properties. Furthermore, it is shown that with 99% probability, one HiperLAN/2 channel could provide capacity above 170 Mbits/s. In Fig. 7, the capacity for the whole channel is presented. It is shown that for with 99% probability, the channel capacity for the whole 120 MHz MIMO channel is above 1150 Mbit/s (larger than 170x6 Mbit/s). This means that there is also some frequency diversity gain in such cases, see also [14].

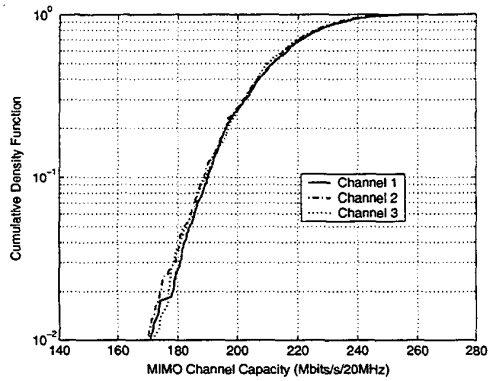


**Fig. 6.** CDF of 20 MHz MIMO Channel Capacity. Power is equally allocated, the SNR at the receiver side is 20dB

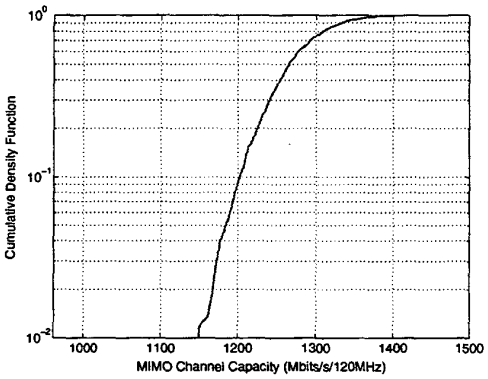


**Fig. 7.** CDF of 120 MHz MIMO Channel Capacity. Power is equally allocated, the SNR at the receiver side is 20dB

## 5. CONCLUSIONS

In this paper, we study the statistical characteristics of NLOS Indoor MIMO channels based on 5.2 GHz measurements. It is shown that the average power delay profile follows the exponentially decaying curve and for each tap, the channel covariance matrix can be well approximated by the Kronecker product of the covariance matrices at both sides respectively. We propose a wideband model based on these results and Monte-Carlo simulations show reasonably good agreement between our model and the measured data. We also use this model to simulate HiperLAN/2 channels.

## 6. REFERENCES

[1] G. J. Foshini, "Layered space-time architecture for wireless communication in a fading environment when using multiple antennas," *Bell Laboratories Technical Journal*, vol. 1, no. 2, pp. 41–59, Autumn 1996.

[2] I. Emre Telatar, "Capacity of multi-antenna Gaussian channels," *European Transactions on Telecommunications*, vol. 10, no. 6, pp. 585–595, Nov./Dec. 1999.

[3] K. I. Pedersen, J. B. Andersen, J. P. Kermoal, and P. Mogensen, "A stochastic Multiple-Input-Multiple-Output radio channel model for evaluation of space-time coding algorithms," in *Proceedings IEEE Vehicular Technology Conference*. Fall, 2000, pp. 893–897.

[4] Kai Yu, Mats Bengtsson, Björn Ottersten, Peter Karlsson, Darren McNamara, and Mark Beach, "Measurement analysis of NLOS indoor MIMO channels," in *Proceedings IST Mobile Communications Summit, Barcelona, Spain*, September 2001, pp. 277–282.

[5] Kai Yu, Mats Bengtsson, Björn Ottersten, Darren McNamara, Peter Karlsson, and Mark Beach, "Second order statistics of NLOS indoor MIMO channels based on 5.2 GHz measurements," in *Proceedings IEEE Globecom 2001, San Antonio, Texas, USA*, November 2001, vol. 1, pp. 156–160.

[6] D. Gesbert, H. Bölcskei, D. Gore, and A. Paulraj, "MIMO wireless channels: capacity and performance," in *Proceedings Global Telecommunications Conference*, November 2000, vol. 2, pp. 1083–1088.

[7] Da-Shan Shiu, G. J. Foschini, M. J. Gans, and J. M. Kahn, "Fading correlation and its effect on the capacity of multielement antenna systems," *IEEE Transactions on Communications*, vol. 48, no. 3, pp. 502–513, March 2000.

[8] Akbar Sayeed, "Modeling and capacity of realistic spatial MIMO channels," in *Proceedings of IEEE International Conference on Acoustics, Speech, and Signal Processing*, 2001, vol. 4, pp. 2489 –2492.

[9] D. P. McNamara, M. A. Beach, P. N. Fletcher, and P. Karlsson, "Initial investigation of multiple-input multiple-output channels in indoor enviroments," in *Proceedings IEEE Benelux Chapter Symposium on Communications and Vehicular Technology, Leuven, Belgium*, October 2000.

[10] D. P. Palomar, J. R. Fonollosa, and M. A. Lagunas, "Capacity results of spatially correlated frequency-selective MIMO channels in UMTS," in *Proceedings IEEE Vehicular Technology Conference*. IEEE VTC Fall, 2001, pp. 553 – 557.

[11] Theodore S. Rappaport, *Wireless Communications, Principles and Practice*, Prentice Hall PTR, 1996.

[12] Gene H. Golub and Charles F. Van Loan, *Matrix Computations*, The Johns Hopkins University Press, London, 3rd edition, 1996.

[13] J. Medbo, H. Andersson, P. Schramm, H. Asplund, and J. E. Berg, "Channel models for HIPERLAN/2 in different indoor scenarios," *COST259 TD(98)70*, April 1998.

[14] A. F. Molisch, M. Steinbauer, M. Toeltsch, E. Bonek, and R. S. Thoma, "Measurement of the capacity of MIMO systems in frequency selective channels," in *Proceedings IEEE Vehicular Technology Conference*. IEEE VTC Spring, 2001.